

Revision #2

Raman spectroscopy and the inversion degree of natural Cr-bearing spinels

Davide Lenaz^{1*} Vanni Lughi²

¹ *Department of Mathematics and Geosciences, University of Trieste, Trieste, I-34127 Italy;*

lenaz@units.it

² *Department of Engineering and Architecture, University of Trieste, Trieste, I-34127 Italy*

Abstract

Natural Cr-spinels already characterized by X-ray single crystal diffraction and electron microprobe have been analyzed by Raman spectroscopy. The results we report show that there is a strong correlation between the Cr/(Cr+Al) ratio (Cr#) and the A_{1g} mode for the studied spinels. A strong correlation of this mode with Mg/(Mg+Fe²⁺) (Mg#) can be seen only for spinels with Mg# higher than 0.60. Other modes can increase, decrease or disappear depending on the Cr#. Among the spinels with low Cr# it is possible to define their order/disorder degree. In fact, spinels with an inversion degree lower than 0.14 show an E_g mode at about 400-410 cm^{-1} , while spinels with Cr# higher than 0.20 register the appearance of a peak in the region 150-200 cm^{-1} , while other peaks are substituted by smooth curves. The results show that the use of Raman applied to spinel in provenance studies cannot yield a 100% confidence because of the uncertainties in the relation between Mg# and the different modes.

Keywords Raman spectroscopy; natural spinels; order/disorder; provenance study

Introduction

Spinel and spinel-like minerals are subjects of continuous scientific interest and have been deeply investigated in both earth science and materials sciences, because of their interesting properties as pigments, refractory materials, semi-conductors, catalysts and batteries. In nature they occur in basic-ultrabasic plutonic rocks, in mantle derived rocks, in different metamorphic occurrences and, due to their high hardness and resistance to alteration, they are also a common detrital constituent of sedimentary rocks (Irvine 1967; Dick and Bullen 1984; Lenaz et al. 2000; Barnes and Roeder 2001; Kamenetsky et al. 2001). The spinel family is cubic, $Fd-3m$, with a very compact oxygen array and the cations in tetrahedral (T) and octahedral (M) coordination. According to Lindsley (1976), Hill *et al.* (1979) and Waychunas (1991) the cubic cell has 96 sites, 64 are T-sites and 32 are M-sites, but only 24 are occupied. Chemically, spinel may be described by the ${}^{IV}(A_{1-i}B_i){}^{VI}(B_{2-i}A_i)O_4$ structural formula, where IV and VI represent tetrahedrally and octahedrally coordinated sites, A and B are cations with variable valence distributed in T and M sites and i is the inversion parameter. At low temperature, there are two ordered configurations, one with $i=0$ (normal spinel; e.g. $MgAl_2O_4$, $Fe^{2+}Al_2O_4$, $MgCr_2O_4$, $Fe^{2+}Cr_2O_4$) meaning that divalent cations enter the T site and trivalent cations the M one, and another with $i=1$ (inverse spinel; e.g. $MgFe^{3+}_2O_4$, $Fe^{2+}Fe^{3+}_2O_4$). Anyway, disorder can occur at increasing temperature, leading to inter-site exchange of A and B cations over the three cation sites per formula unit modifying the M-O and T-O bond distances. In the spinel cell, the oxygen atom is linked to three octahedral cations and one tetrahedral cation lying on opposite sides of the oxygen layer, respectively, to form a trigonal pyramid. Movement of the oxygen atom along the cube diagonal [111] causes the oxygen layers in the spinel structure to be slightly puckered so that variations in u correspond to displacements of the oxygens along the cube diagonal, reflecting adjustments to the relative effective radii of cations in the tetrahedral and octahedral sites. An increase in u corresponds to an enlargement

of the tetrahedral coordination polyhedra and a compensating decrease in the octahedra (Lindsley 1976).

Several studies in the past years took into consideration natural and synthetic spinels with different compositions (Malézieux et al. 1983; Malézieux and Piriou 1988; Wang et al. 2002a; among the others) and/or on specific topics such as the variations of Raman spectra within a solid solution series (Lenaz and Lughì 2013; Lenaz and Skogby 2013), with pressure MgCr_2O_4 (Wang et al 2002b; Yong et al 2012); Fe_2TiO_4 (Kyono et al 2011); MgFe_2O_4 (Wang et al 2002a; Winell et al 2006), temperature MgAl_2O_4 (Slotznick and Shim 2008) and ordering (Minh and Yang 2004). D'Ippolito et al. (2015) studied synthetic spinel single crystals, having compositions approaching chromate, aluminate, and ferrite spinel end-members, to identify Raman peculiarities of each endmember and showed how substitution of the divalent and trivalent cations affects the Raman modes.

Even if Cr-bearing spinels typically occur as accessory phases, they are widely considered as petrogenetic indicators as systematic relationships exist between spinel chemistry and bulk-rock composition or mineral assemblage, and geological environment and process (Irvine 1967; Dick & Bullen 1984; Lenaz et al. 2000; Barnes and Roeder 2001; Kamenetsky et al. 2001) so that, among the different spinels, those bearing chromium are among the most important because of their geological occurrence spanning from the Earth interior, being frequently included in diamonds (Sobolev 1977; Barnes and Roeder 2001; Lenaz et al. 2009a, 2013) and in mantle xenoliths, to the extraterrestrial space (Bunch et al. 1967; Wlotzka 2005; Heck et al. 2010; Karwowski et al. 2013; Schmitz 2013; Lenaz et al. 2015). Moreover it is the ore mineral for Cr and because it is related to PGE (Platinum Group Elements) extraction (Hutchinson et al. 2015; Kamenetsky et al. 2015; Uysal et al. 2015 among the most recent). For these reasons and because it is highly resistant to low-grade alteration, mechanical weathering and breakdown, Cr-spinel is widely used as an important tool for paleogeographic

reconstructions (Cookenboo et al. 1997; Lenaz et al. 2003, 2009b; Barkov et al. 2013; Schmitz et al. 2014, 2015; Gawlik et al. 2015 among the others).

Previous Raman studies include works by Wang et al. (2004a; 2004b) on meteorite spinels, Reddy and Frost (2005) in mafic rocks and Zhang and Gan (2011). In all natural spinels and almost all of the synthetic ones, even if the vibrational modes are easily assigned, the presence of several cations within the structure has generated difficulties of interpretation of the Raman shifts due to the possibility for several cations to enter the octahedral and tetrahedral sites.

The aim of this work is to study by means of Raman spectroscopy, Cr-spinel single crystals previously characterized by means of single crystal X-ray diffraction and electron microprobe. In such a way we should be able to verify how different Raman shifts can be attributed to the presence of the different cations in the sites and consequently verify the effects of the cation order-disorder phenomena. Moreover we will verify if Raman spectroscopy could be a valuable technique to characterize Cr-spinel in provenance studies, i.e. we will see if any of the Raman mode could be related to the most used chemical indexes for Cr-spinels as Cr# ($\text{Cr}/(\text{Cr}+\text{Al})$) and Mg# ($\text{Mg}/(\text{Mg}+\text{Fe}^{2+})$).

Materials and methods

One of the commonly used values to classify Cr-spinels is the Cr/(Cr+Al) ratio, i.e. Cr#, that is related to the geological occurrence of the spinel. In order to have the most complete series of Cr-spinels we selected spinels from mantle xenoliths from Libya and Cameroon (LB1, LB3, LB10, LB16 and BAR; Lenaz unpublished data), alpine peridotite (R2 and R6, Ronda massif, Lenaz et al. 2010), ophiolites (C1 and AV1, Shetland Islands, Derbyshire et al. 2013), layered complexes (SWLB2, Stillwater, Lenaz et al. 2012; U392, Greenland, Lenaz unpublished), included in diamond (UDK5, Lenaz et al. 2009a).

Spinel from mantle xenoliths have Cr# lower than 0.20. For the range 0.20-0.60 we selected spinels from alpine peridotite and Stillwater complex. Spinel with Cr# higher than 0.60 are from Shetland Isl. and included in diamond. Complete structural and chemical analyses are reported in the above cited papers, while a summary of the values useful for the purpose of this paper are reported in Table 1. The studied spinels show the following approximate compositions: LB1 ($\text{Mg}_{0.79}\text{Fe}^{2+}_{0.20}\text{Al}_{1.81}\text{Cr}_{0.15}\text{Fe}^{3+}_{0.03}\text{O}_4$), LB3 ($\text{Mg}_{0.76}\text{Fe}^{2+}_{0.23}\text{Al}_{1.57}\text{Cr}_{0.36}\text{Fe}^{3+}_{0.06}\text{O}_4$), LB10 ($\text{Mg}_{0.80}\text{Fe}^{2+}_{0.19}\text{Al}_{1.74}\text{Cr}_{0.23}\text{Fe}^{3+}_{0.03}\text{O}_4$), LB16 ($\text{Mg}_{0.79}\text{Fe}^{2+}_{0.20}\text{Al}_{1.71}\text{Cr}_{0.25}\text{Fe}^{3+}_{0.03}\text{O}_4$), BAR ($\text{Mg}_{0.82}\text{Fe}^{2+}_{0.18}\text{Al}_{1.77}\text{Cr}_{0.17}\text{Fe}^{3+}_{0.05}\text{O}_4$), R2 ($\text{Mg}_{0.72}\text{Fe}^{2+}_{0.28}\text{Al}_{1.45}\text{Cr}_{0.53}\text{Fe}^{3+}_{0.01}\text{O}_4$), R6 ($\text{Mg}_{0.64}\text{Fe}^{2+}_{0.36}\text{Al}_{1.16}\text{Cr}_{0.75}\text{Fe}^{3+}_{0.06}\text{O}_4$), C1 ($\text{Mg}_{0.53}\text{Fe}^{2+}_{0.46}\text{Al}_{0.35}\text{Cr}_{1.55}\text{Fe}^{3+}_{0.08}\text{O}_4$), AV1 ($\text{Mg}_{0.50}\text{Fe}^{2+}_{0.49}\text{Al}_{0.75}\text{Cr}_{1.21}\text{Fe}^{3+}_{0.04}\text{O}_4$), SWLB2 ($\text{Mg}_{0.47}\text{Fe}^{2+}_{0.53}\text{Al}_{0.76}\text{Cr}_{1.10}\text{Fe}^{3+}_{0.11}\text{O}_4$), U392 ($\text{Mg}_{0.44}\text{Fe}^{2+}_{0.55}\text{Al}_{0.45}\text{Cr}_{1.34}\text{Fe}^{3+}_{0.20}\text{O}_4$), UDK5 ($\text{Mg}_{0.61}\text{Fe}^{2+}_{0.38}\text{Al}_{0.25}\text{Cr}_{1.70}\text{Fe}^{3+}_{0.05}\text{O}_4$).

The Raman spectra were collected by a Renishaw InVia Spectrometer (objective 50x with 0.75 NA, 1200 lines/mm grating, 576 pixel CCD detector). The excitation was a near-infrared diode laser at 785 nm excitation, delivering 16 mW at the sample surface, focused on a spot of approximately $10\ \mu\text{m}^2$.

Results and discussion

In spinels there are five Raman-active modes, i.e. $A_{1g} + E_g + 3F_{2g}$. Spinel oxides exhibit Raman vibrational modes in the $100\text{-}800\ \text{cm}^{-1}$ spectral region. Strong bands are observed in the region around $400\text{-}500\ \text{cm}^{-1}$ and $700\text{-}800\ \text{cm}^{-1}$. These modes are assigned to the E_g and A_{1g} modes, respectively. The bands around $600\ \text{cm}^{-1}$ are assigned to the third F_{2g} symmetry species, the bands around $480\text{-}520\ \text{cm}^{-1}$ to the second F_{2g} symmetry species, whereas, the bands around $200\text{-}300\ \text{cm}^{-1}$ are assigned to the first F_{2g} symmetry species (D'Ippolito et al. 2015 and references therein).

Although there has been a large amount of experimental work on pure spinels, the literature is inconsistent with regard to the assignment of the specific atomic motions within the spinel lattice during the Raman-active vibrations, in fact the A_{1g} mode in literature has been assigned to:

1. The symmetric breathing mode of the AO_4 unit within the spinel lattice. Cynn et al. (1992) argued that the oxygen atoms move away from the tetrahedral cation along the direction of the bonds. Neither the tetrahedral nor octahedral cations are in motion during this vibration.
2. The symmetric breathing mode of the octahedral unit (Marinković Stanojević et al. 2007);
3. The random occupation of the octahedral sites by the A^{2+} and B^{3+} cations (Laguna-Bercero et al. 2007);
4. The stretching of AlO_4 tetrahedra (Barpanda et al. 2006).

The main differences among the aluminates, chromates, and ferrites have been explored by D'Ippolito et al. (2015) and concern the A_{1g} , $F_{2g(3)}$ and E_g modes. These three modes have been assigned to different movements of the oxygen atoms along the T–O bond. Each tetrahedron shares oxygen with three octahedra; thus, even if the octahedral cation remains at rest, the nature of the M cation must influence the M–O bonding force causing a change of the oxygen position along the M–O–T direction. Those authors suggest that simply analyzing the E_g peak position, it is possible to obtain information on which subgroup a spinel belongs to, because an E_g mode at $\sim 450\text{ cm}^{-1}$ is distinctive of chromate spinels, an E_g mode at $\sim 400\text{ cm}^{-1}$ is distinctive of aluminate spinels, and an E_g mode below 380 cm^{-1} is distinctive of ferrite spinels.

Spinel with Cr# > 0.60

The main aspects of spinels with such an high Cr# is that the Cr cation consistently fill the octahedral site ($1.2 < Cr < 1.7$ atoms per formula unit, apfu). The Mg#, i.e. $Mg/(Mg+Fe^{2+})$, is in the range 0.45-

0.62. According to Urusov (1983), for chromium-containing spinels the large excess octahedral crystal field stabilization energy of Cr^{3+} ($\Delta \text{CFSE}_{(\text{oct-tet})} \approx 160 \text{ kJ/mol}$; O'Neill and Navrotsky 1984) should ensure that Cr-bearing spinels have an almost completely normal cation distribution; consequently, high amounts of chromium should act as a “buffer” preventing the exchange of the other cations within the T and M site (Lenaz et al. 2004). As a consequence the inversion degree is lower than 0.05. For these spinels the oxygen positional parameter is in the range 0.2620-0.2629 being a function of the Cr# (Lenaz et al. 2011).

Spectra are not very well defined and present a large peak at about 700 cm^{-1} , one at 650 cm^{-1} and other peaks at about 460 cm^{-1} (Fig. 1). Synthetic Mg-chromite and chromite presents the A_{1g} mode at about 684 and 674 cm^{-1} , respectively (Lenaz and Lughì 2013), while an increase of Al content in the M site yields to a shift of this mode to higher frequencies being about 748 for hercynite and 768 for spinel s.s.. The peak at 650 cm^{-1} could be related to the $F_{2g(3)}$ peak that in the $(\text{Mg,Fe})\text{Cr}_2\text{O}_4$ spinels is in the range 628 - 640 cm^{-1} (Lenaz and Lughì 2013). The one at 460 cm^{-1} is possibly the E_g peak. Even if this last peak is not well defined it confirms the observation by D'Ippolito et al. (2015) that chromate spinels can be recognized by the E_g peak at about 450 cm^{-1} .

Spinel with $0.20 < \text{Cr\#} < 0.60$

The Cr content is variable in the range 0.5-1.1 apfu, while the Mg# is within 0.47-0.72. Even if the amount of Cr cannot be very high, the inversion degree is still low, being in the range 0.02-0.07. The u value is in the range 0.2630-0.2635. As stated by Lenaz et al. (2010), even in this case this parameter is somehow linked to the Cr#.

These spinels are characterized by the presence of a large peak in the range 700 - 730 cm^{-1} . As seen above this is the A_{1g} mode. The shift of this peak is a consequence of the higher amount of Al in the M site substituting Cr. The $F_{2g(3)}$ peak is present at about 620 cm^{-1} . According to D'Ippolito et al. (2015)

the hercynite F_{2g} peak is at 617 cm^{-1} . Notably the peak decrease its intensity with the increase of the Cr#, and the consequent decrease of the hercynite content in the studied spinels. Other peaks, that are not very well defined, are in the range $500\text{-}550\text{ cm}^{-1}$, $450\text{-}500\text{ cm}^{-1}$ and $300\text{-}350\text{ cm}^{-1}$. While the first can be related to the $F_{2g(2)}$ peak, the others show a character resembling the E_g peaks noticed by D'Ippolito et al. (2015) and suggesting a certain degree of inversion. It is not possible to decipher if these natural spinels are chromate, aluminate or ferrite spinels by means of the E_g mode as suggested by D'Ippolito et al. (2015).

Spinel with Cr#<0.20

The chromium content of these spinels is quite low being in the range 0.15-0.36 apfu. The Mg# is higher than that of the other studied spinels (0.77-0.83). From a structural point of view, the oxygen positional parameter, u , is comprised between 0.26237 (7) and 0.26345 (5) (Lenaz unpublished data). This fact means that they are differently ordered. In particular, spinels having high u values has an inversion degree, i , in the range 0.12-0.14 while those with low u values show an inversion degree equal to 0.20-0.21. Princivalle et al. (1989) argued that within a single suite of mantle xenoliths, the ratio of the M-O to T-O bond lengths, and consequently u , are constant, despite important changes in composition. The u values is related to the cooling history of the spinels.

The spinels with i lower than 0.14 are characterized by an intense peak at $739\text{-}753\text{ cm}^{-1}$. This peak moves towards higher values of Raman shift with the decrease of Cr#. Moreover, with the same Cr# decrease, the peak intensity also decreases. The same features are also recognizable for the broad peaks in the range $600\text{-}650\text{ cm}^{-1}$. An opposite behavior occurs for the peak in the range $395\text{-}410\text{ cm}^{-1}$, which grows more intense and sharper as the Cr# value decreases. Notably the characteristic E_g peak of the MgAl_2O_4 spinel has a value of 408 cm^{-1} (D'Ippolito et al. 2015) so that it is quite clear that the decrease of chromium in the spinel yield to an higher spinel s.s. molecule. Spinel with an inversion degree

higher than 0.2 are characterized by the presence of a smooth peak at values in the range 150-200 cm^{-1} . Peaks in that range are related to the inversion in FeAl_2O_4 and MnAl_2O_4 spinels or are characteristic of ZnCr_2O_4 (D'Ippolito et al. 2015). The same, but with much lower intensities, has also been observed in MgCr_2O_4 and FeCr_2O_4 (Lenaz and Lughì 2013). These aspects seem rather interesting because that peak seems to appear only in pure chromate or in aluminate spinels where the divalent cation present an high T-O bond length ($\text{Fe}^{2+} = 2.000$; $\text{Mn}^{2+} = 2.036$; Lavina et al. 2002). Comparison with data and suggestions by D'Ippolito et al. (2015) confirms that the spinels with low Cr content (Cr_2O_3 lower than 20 wt. %) can be similar to aluminate but only if they are well ordered. Disordered spinels do not show a clear E_g mode in the position suggested by those authors.

Implications

In order to verify if Raman spectroscopy can be useful in provenance studies for spinels we analyzed about 150 more spinels from the same occurrences already analyzed by electron microprobe. When working on the provenance of spinels the most useful diagrams to assign them to a proper tectonic setting are the Cr# vs. Mg# (Dick and Bullen 1984; Barnes and Roeder 2001 among the others), the Cr# vs. TiO_2 (Jan and Windley 1990; Arai 1992), the TiO_2 vs. Al_2O_3 (Lenaz et al. 2000; Kamenetsky et al. 2001) or the triangular plot of the trivalent cations Cr, Al and Fe^{3+} . Usually the content of titanium is quite low so that a Raman spectra should be unable to measure its influences on the shift. Consequently we focused our attention on the relations between the Cr# and Mg# with the Raman shift. Considering that in the natural Cr-spinels there are many peaks disappearing or appearing according to the peculiar chemistry or inversion degree of the spinel themselves, our findings suggest that there is a good correlation between the Cr# and the A_{1g} peak mode ($R^2=0.98$), while the relation between Mg# and the A_{1g} is poorer ($R^2=0.73$) because there is a large scattering of data for Mg# lower than 0.6 (Fig. 4). The only other existing correlation could be seen between Cr# and F_{2g} , but it is not very good ($R^2=0.85$)

(Fig. 5). It seems that it should be easy to assign the proper provenance to spinels with high Mg# and low Cr# according to their A_{1g} mode. For spinels with higher Cr# it will be possible to find out the correct Cr# but not the proper Mg# due to scattering of the data. Given this it could be said that Raman spectroscopy applied to spinels has a limited reliability in provenance studies.

Acknowledgments The authors kindly acknowledge the Spectroscopy Laboratory of the Department of Engineering and Architecture, University of Trieste, where the Raman measurements have been carried out. DL thanks FRA2013 funding from University of Trieste. Kristina Lilova for editorial handling and two anonymous reviewer for their comments are kindly acknowledged.

References

- Arai, S. (1992) Chemistry of chromian spinel in volcanic rockj as a potential guide to magma chemistry. *Mineralogy Magazine*, 56, 173-184.
- Barkov, A.Y., Nixon, G.T., Levson, V.M., Martin, R.F., and Fleet, M.E. (2013) Chromian spinel from PGE-bearing placer deposits, Britishh Columbia, Canada: mineralogical associations and provenance. *Canadian Mineralogist*, 51, 501-536.
- Barnes, S.J., and Roeder, P.L. (2001) The range of spinel compositions in terrestrial mafic and ultramafic rocks. *Journal of Petrology*, 42, 2279–2302.
- Barpanda, P., Behera, S.K., Gupta, P.K., Pratihar, S.K., and Bhattacharya, S. (2006) Chemically induced order disorder transition in magnesium aluminium spinel. *Journal of the European Ceramic Society*, 26, 2603-2609.
- Bunch, T.E., Keil, K., and Snetsinger, K.G. (1967) Chromite composition in relation to chemistry and texture of ordinary chondrites. *Geochimica et Cosmochimica Acta*, 31, 1569-1582.

- Cookenboo, H.O., Bustin, R.M., and Wilks, K.R. (1997) Detrital chromian spinel compositions used to reconstruct the tectonic setting of provenance: implications for orogeny in the Canadian Cordillera. *Journal of Sedimentary Petrology*, 67, 116-123.
- Cynn, H., Sharma, S.K., Cooney, T.F., and Nicol, M. (1992) High-temperature Raman investigation of order-disorder behavior in the $MgAl_2O_4$ spinel. *Physical Review B*, 45, 500-502.
- D'Ippolito, V., Andreozzi, G.B., Bersani, D., and Lottici, P.P. (2015) Raman fingerprint of chromate, aluminate and ferrite spinels. *Journal of Raman Spectroscopy*, 46, 1255–1264.
- Derbyshire, E.J., O'Driscoll, B., Lenaz, D., Gertisser, R., and Kronz, A. (2013) Compositional heterogeneity in chromitite seams from the Shetland Ophiolite Complex (Scotland): implications for chromitite petrogenesis and late-stage alteration in the upper mantle portion of a supra-subduction zone ophiolite. *Lithos*, 162-163, 279-300.
- Dick, H.J.B., and Bullen, T. (1984) Chromian spinel as a petrogenetic indicator in abyssal and alpine-type peridotites and spatially associated lavas. *Contributions to Mineralogy and Petrology*, 86,54-76.
- Gawlick, H.-J., Aubrecht, R., Schlagintweit, F., Missoni, S., and Plašienka, D. (2015) Ophiolitic detritus in Kimmeridgian resedimented limestones and its provenance from an eroded obducted ophiolitic nappe stack south of the Northern Calcareous Nappe (Austria). *Geologica Carpathica*, 66, 473-487.
- Heck, P.R., Ushikubo, T., Schmitz, B., Kita, N.T., Spicuzza, M.J., and Valley, J.W. (2010) A single asteroidal source for extraterrestrial Ordovician chromite grains from Sweden and China: high-precision oxygen three-isotopes SIMS analysis. *Geochimica et Cosmochimica Acta*, 74, 497-509.
- Hill, R.J., Craig, J.R., and Gibbs, G.V. (1979) Systematics of the spinel structure type. *Physics and Chemistry of Minerals*, 4, 317-339.

- Hutchinson, D., Foster, J., Prichard, H., and Gilbert, S. (2015) Concentration of Particulate Platinum-Group Minerals during Magma Emplacement; a Case Study from the Merensky Reef, Bushveld Complex. *Journal of Petrology*, 56, 113–159.
- Irvine, T.N. (1967) Chromian spinel as a petrogenetic indicator. Part 2. Petrologic applications. *Canadian Journal of Earth Sciences*, 4, 71-103.
- Jan, M. Q, and Windley, B. F. (1990) Chromian spinel-silicate chemistry in ultramafic rocks of the Jijal complex, Northwest Pakistan. *Journal of Petrology*, 31, 667-715.
- Kamenetsky, V.S., Crawford, A.J., and Meffre, S. (2001) Factors controlling chemistry of magmatic spinel: an empirical study of associated olivine, Cr-spinel and melt inclusions from primitive rocks. *Journal of Petrology*, 42, 655-671.
- Kamenetsky, V.S., Park, J.-W., Mungall, J.E., Pushkarev, E.V., Ivanov, A.V., Kamenetsky, M.B., and Yaxley, G.M. (2015) Crystallization of platinum-group minerals from silicate melts: Evidence from Cr-spinel-hosted inclusions in volcanic rocks. *Geology*, 43, 903–906.
- Karwowski, Ł., Helios, K., Kryza, R., Muszyński, A., and Drożdżewski, P. (2013) Raman spectra of selected mineral phases of the Morasko iron meteorite. *Journal of Raman Spectroscopy*, 44, 1181-1186.
- Kyono, A., Ahart, M., Yamanaka, T., Gramsch, S., Mao, H.K., and Hemley, R.J. (2011) High-pressure Raman spectroscopic studies of ulvöspinel Fe_2TiO_4 . *American Mineralogist*, 96, 1193-1198.
- Laguna-Bercero, M. A., Sanjuán, M. L., and Merino, R. I. (2007) Raman spectroscopic study of cation disorder in poly- and single crystals of the nickel aluminate spinel. *Journal of Physics: Condensed Matter*, 19, 1–10.
- Lavina, B., Salviulo, G., and Della Giusta, A. (2002) Cation distribution and structure modelling of spinel solid solutions. *Physics and Chemistry of Minerals*, 29, 10–18.

- Lenaz, D., and Lughi, V. (2013) Raman study of MgCr_2O_4 - $\text{Fe}^{2+}\text{Cr}_2\text{O}_4$ and MgCr_2O_4 - $\text{MgFe}_2^{3+}\text{O}_4$ synthetic series: the effects of Fe^{2+} and Fe^{3+} on Raman shifts. *Physics and Chemistry of Minerals*, 40, 491-498.
- Lenaz, D., and Skogby, H. (2013) Structural changes in the FeAl_2O_4 - FeCr_2O_4 solid solution series and their consequences on natural Cr-bearing spinels. *Physics and Chemistry of Minerals*, 40, 587-595.
- Lenaz, D., Kamenetsky, V.S., Crawford, A.J., and Princivalle, F. (2000) Melt inclusions in detrital spinel from SE Alps (Italy-Slovenia): A new approach to provenance studies of sedimentary basins. *Contributions to Mineralogy and Petrology*, 139, 748-758.
- Lenaz, D., Andreozzi, G.B., Mitra, S., Bidyananda, M., and Princivalle, F. (2004) Crystal chemical and ^{57}Fe Mössbauer study of chromite from the Nuggihalli schist belt (India). *Mineralogy and Petrology*, 80, 45-57.
- Lenaz, D., Logvinova, A.M., Princivalle, F., and Sobolev, N.V. (2009a) Structural parameters of chromites included in diamonds and kimberlites from Siberia: A new tool in discriminating different ultramafic sources. *American Mineralogist*, 94, 1067-1070.
- Lenaz, D., Mazzoli, C., Spišiak, J., Princivalle, F., and Maritan, L. (2009b) Detrital Cr-spinel in the Šambron-Kamenica Zone (Slovakia): evidence for an ocean-spreading zone in the Northern Vardar suture? *International Journal of Earth Sciences*, 98, 345-355.
- Lenaz, D., De Min, A., Garuti, G., Zaccarini, F., and Princivalle, F. (2010) Crystal chemistry of Cr-spinels from the lherzolite mantle peridotite of Ronda (Spain). *American Mineralogist*, 95, 1323-1328
- Lenaz, D., Garuti, G., Zaccarini, F., Cooper, R.W., and Princivalle F. (2012) The Stillwater Complex: The response of chromite crystal chemistry to magma injection. *Geologica Acta*, 10, 33-41.

- Lenaz, D., Skogby, H., Logvinova, A.M., Sobolev, N.V., and Princivalle, F. (2013) A micro-Mössbauer study of chromites included in diamond and other mantle-related rocks. *Physics and Chemistry of Minerals*, 40, 671-679
- Lenaz, D., Princivalle, F., and Schmitz, B. (2015) First crystal-structure determination of chromites from an acapulcoite and ordinary chondrites. *Mineralogical Magazine*, 79, 755-765.
- Lindsley, D.H. (1976) The crystal chemistry and structure of oxide minerals as exemplified by the Fe-Ti oxides. Pp. 1-60 in: *Oxide minerals* (D. Rumble III, editor), Mineralogical Society of America, Chelsea, Michigan (USA)
- Malézieux, J.M., Barbillat, J, Cervelle, B, Coutures, J.P., Couzi, M, and Piriou, B (1983) Étude de spinelles de synthèse de la série $Mg(Cr_xAl_{2-x})O_4$ et de chromites naturelles par microsonde Raman-Laser. *TMPM Tschermacks Min Petr Mitt* 32: 171-185
- Malézieux, J.M., and Piriou, B. (1988) Relation entre la composition chimique et le comportement vibrationnel de spinelles de synthèse et de chromites naturelles en microspectrométrie Raman. *Bullettin Minéralogie*, 111, 649-669.
- Marinković Stanojević, Z.V., Romčević, N., and Stojanović, B. (2007) Spectroscopic study of spinel $ZnCr_2O_4$ obtained from mechanically activated $ZnO-Cr_2O_3$ mixtures. *Journal of the European Ceramic Society*, 27, 903-907.
- Minh, N.V., and Yang, I.-S. (2004) A Raman study of cation-disorder transition temperature of natural $MgAl_2O_4$ spinel. *Vibrational Spectroscopy*, 35, 93–96.
- O'Neill, H.St.C., and Navrotsky, A. (1984) Cation distributions and thermodynamic properties of binary spinel solid solutions. *American Mineralogist*, 69, 733–753.
- Princivalle, F., Della Giusta, A., and Carbonin, S. (1989) Comparative crystal chemistry of spinels from some suits of ultramafic rocks. *Mineralogy and Petrology*, 40, 117-126.

- Reddy, B.J., and Frost, R.L. (2005) Spectroscopic characterization of chromite from the Moa-Baracoa Ophiolitic Massif, Cuba. *Spectrochimica Acta Part A*, 61, 1721-1728.
- Schmitz, B. (2013) Extraterrestrial spinels and the astronomical perspective on Earth's geological record and evolution of life. *Chemie der Erde*, 73, 113-135.
- Schmitz, B., Huss, G.R., Meiera, M.M.M., Peucker-Ehrenbrink, B., Church, R.P., Cronholm, A., Davies, M. B., Heck, P.R., Johansen, A., Keil, K., Kristiansson, P., Ravizza, G., Tassinari, M. and Terfelt, F. (2014) A fossil winonaite-like meteorite in Ordovician limestone: A piece of the impactor that broke up the L-chondrite parent body? *Earth and Planetary Science Letters*, 400, 145–152.
- Schmitz, B., Boschi, S., Cronholm, A., Heck, P.R., Monechi, S., Montanari, A., and Terfelt, F. (2015) Fragments of Late Eocene Earth-impacting asteroids linked to disturbance of asteroid belt. *Earth and Planetary Science Letters*, 425, 77-83.
- Slotznick, S.P., and Shim, S.H. (2008) In situ Raman spectroscopy measurements of $MgAl_2O_4$ spinel up to 1400 °C. *American Mineralogist*, 93, 470-476.
- Sobolev, N.V. (1977) Deep-seated inclusions in kimberlites and the problem of the compositions of the upper mantle. American Geophysical Union, Washington, D.C. Translated by D.A. Brown from Russian edition (1974). Novosibirsk, Russia, Nauka (in Russian).
- Urusov, V.S. (1983) Interaction of cation on octahedral and tetrahedral sites in simple minerals. *Physics and Chemistry of Minerals*, 9, 1-5.
- Uysal, I., Akmaz, R.M., Kapsiotis, A., Demir, Y., Saka, S., Avcı, E., and Müller, D. (2015) Genesis and geodynamic significance of chromitites from the Orhaneli and Harmancık ophiolites (Bursa, NW Turkey) as evidenced by mineralogical and compositional data. *Ore Geology Reviews*, 65, 26–41.
- Wang, A, Kuebler, K.E., Jolliff, B.L., and Haskin, L.A. (2004b) Raman spectroscopy of Fe-Ti-Cr oxides, case study: Martian meteorite EETA 79001. *American Mineralogist*, 89, 665-680.

- Wang, A., Kuebler, K.E., Jolliff, B.L., and Haskin, L.A. (2004a) Mineralogy of a Martian meteorite as determined by Raman spectroscopy. *Journal of Raman Spectroscopy*, 35, 504-514.
- Wang, Z., Lazor, P., Saxena, S.K., and O'Neill, H.St.C. (2002a) High pressure Raman spectroscopy of ferrite MgFe_2O_4 . *Materials Research Bulletin*, 37, 1589-1602.
- Wang, Z., O'Neill, H.St.C., Lazor, P., and Saxena, S.K. (2002b) High pressure Raman spectroscopic study of spinel MgCr_2O_4 . *Journal of Physics and Chemistry of Solids*, 63, 2057-2061.
- Waychunas, G.A. (1991) Crystal chemistry of oxides and oxyhydroxides. Pp. 11-68 in: *Oxide minerals: petrologic and magnetic significance* (Lindsley, D.H., editor), Mineralogical Society of America, Chelsea, Michigan (USA).
- Winell, S., Annersten, H., and Prakapenka, V. (2006) The high-pressure phase transformation and breakdown of MgFe_2O_4 . *American Mineralogist*, 91, 560-567.
- Wlotzka, F. (2005) Cr spinel and chromite as petrogenetic indicators in ordinary chondrites: equilibration temperatures of petrologic types 3.7 to 6. *Meteoritics & Planetary Science*, 40, 1673-1702.
- Yong, W., Botis, S., Shieh, S.R., Shi, W., and Withers, A.C. (2012) Pressure-induced phase transition study of magnesiocromite (MgCr_2O_4) by Raman spectroscopy and X-ray diffraction. *Physics of the Earth and Planetary Interiors*, 196-197, 75-82.
- Zhang, Z.W., and Gan, F.X. (2011) Analysis of the chromite inclusions found in nephrite minerals obtained from different deposits using SEM-EDS and LRS. *Journal of Raman Spectroscopy*, 42, 1808-1811.

Figure captions

Fig. 1. Raman shifts of the spinels with $\text{Cr}\# > 0.60$. Y axis in arbitrary units

Fig. 2. Raman shifts of the spinels with $0.20 < \text{Cr}\# < 0.60$. Y axis in arbitrary units

Fig. 3. Raman shifts of the spinels with Cr# < 0.20. Top diagram, inversion degree < 0.14. Bottom diagram, inversion degree > 0.20. Y axis in arbitrary units

Fig. 4. Cr# (full circle) vs. A_{1g} mode and Mg# (open circle) vs. A_{1g} mode.

Fig. 5. Cr# vs. F_{2g} mode.

Figure 1

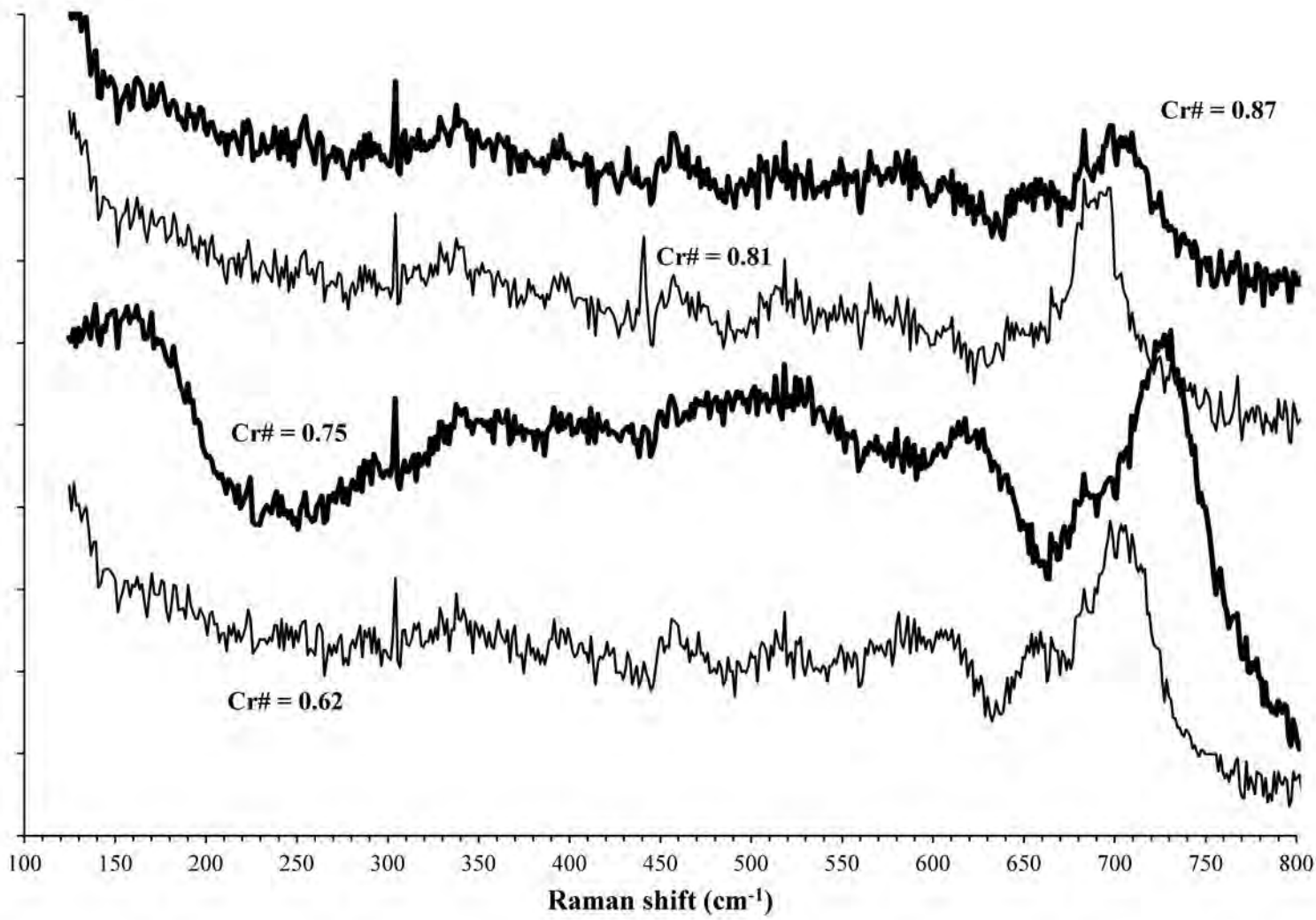


Figure 2

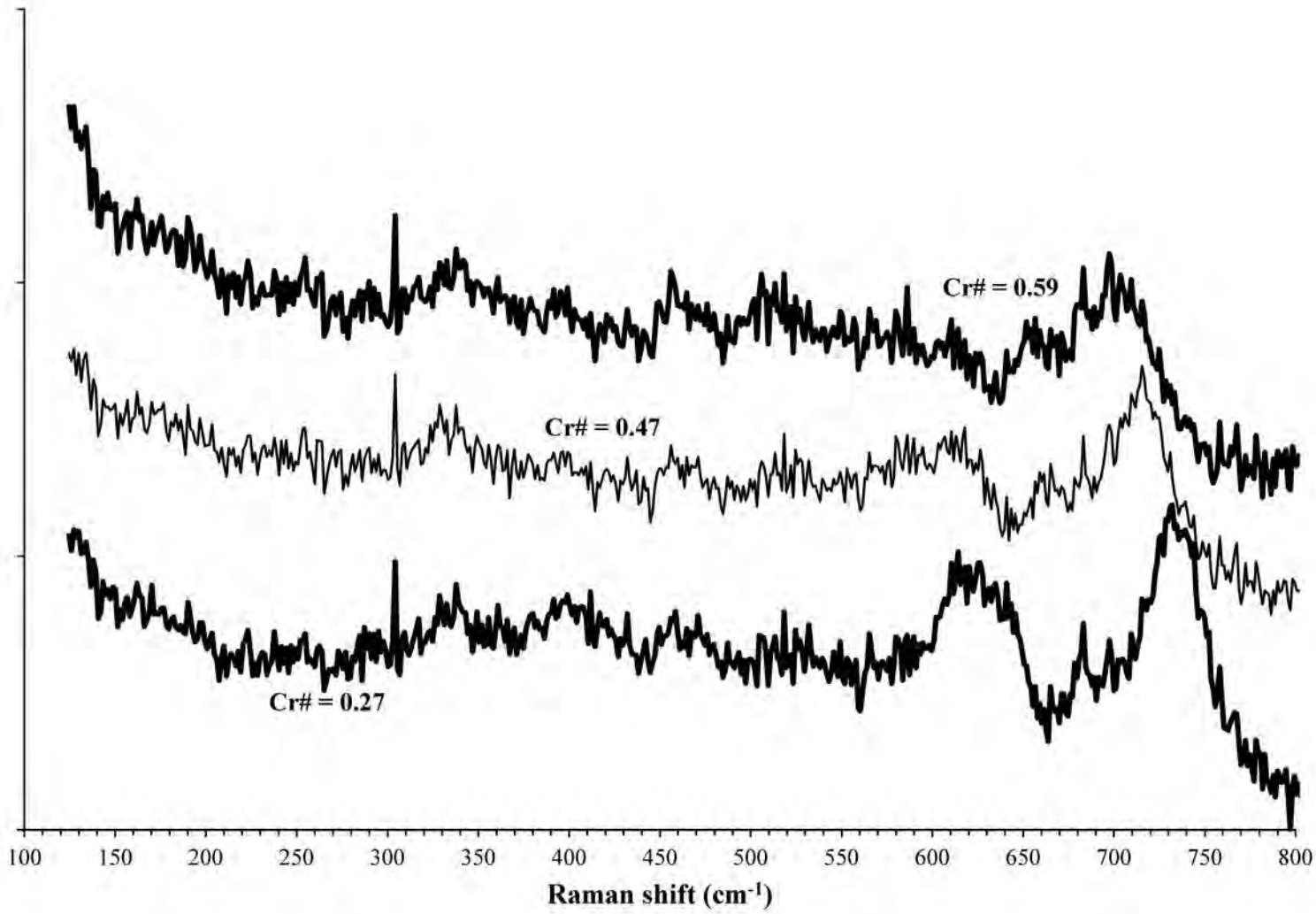


Figure 3

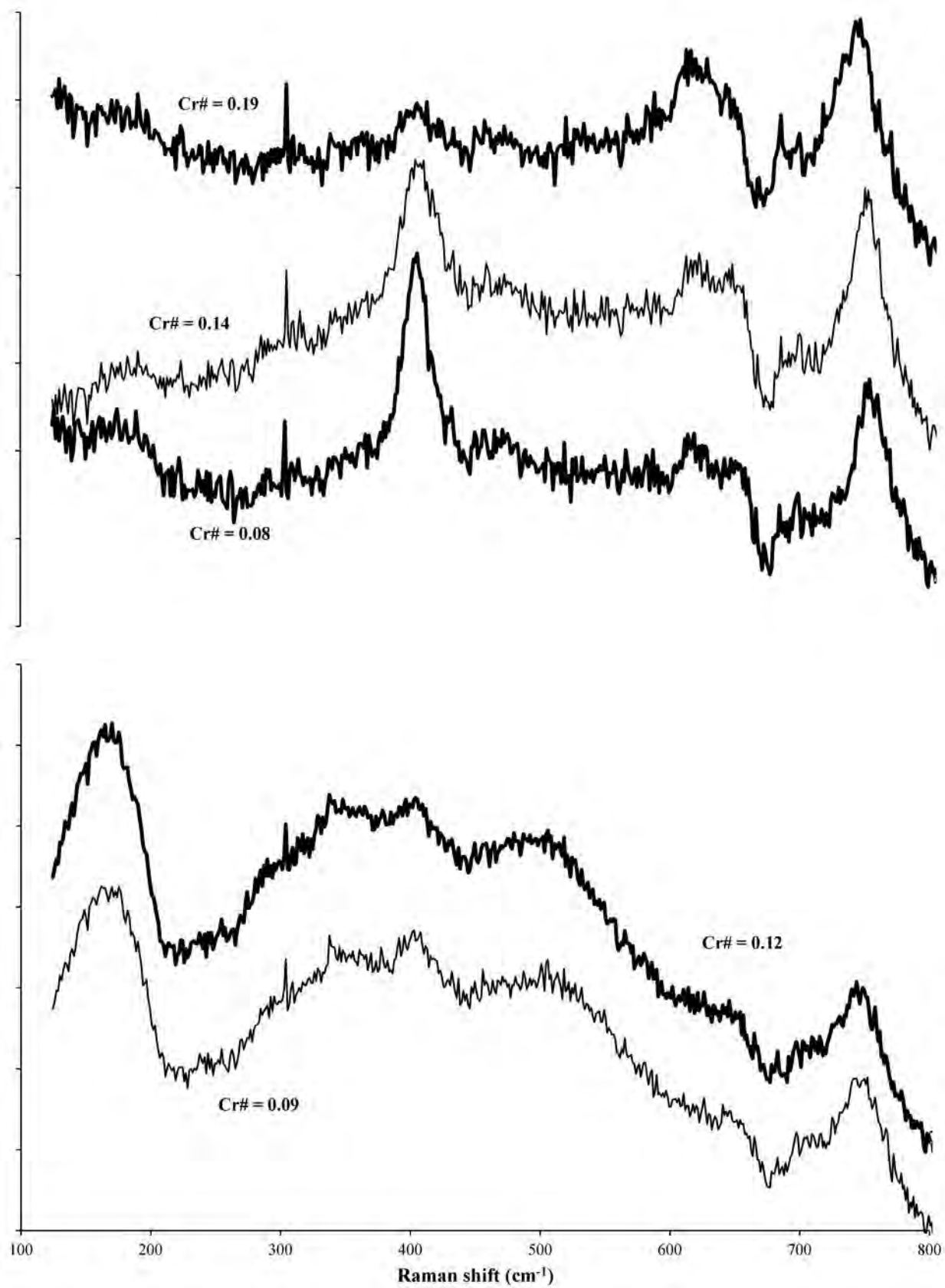


Figure 4

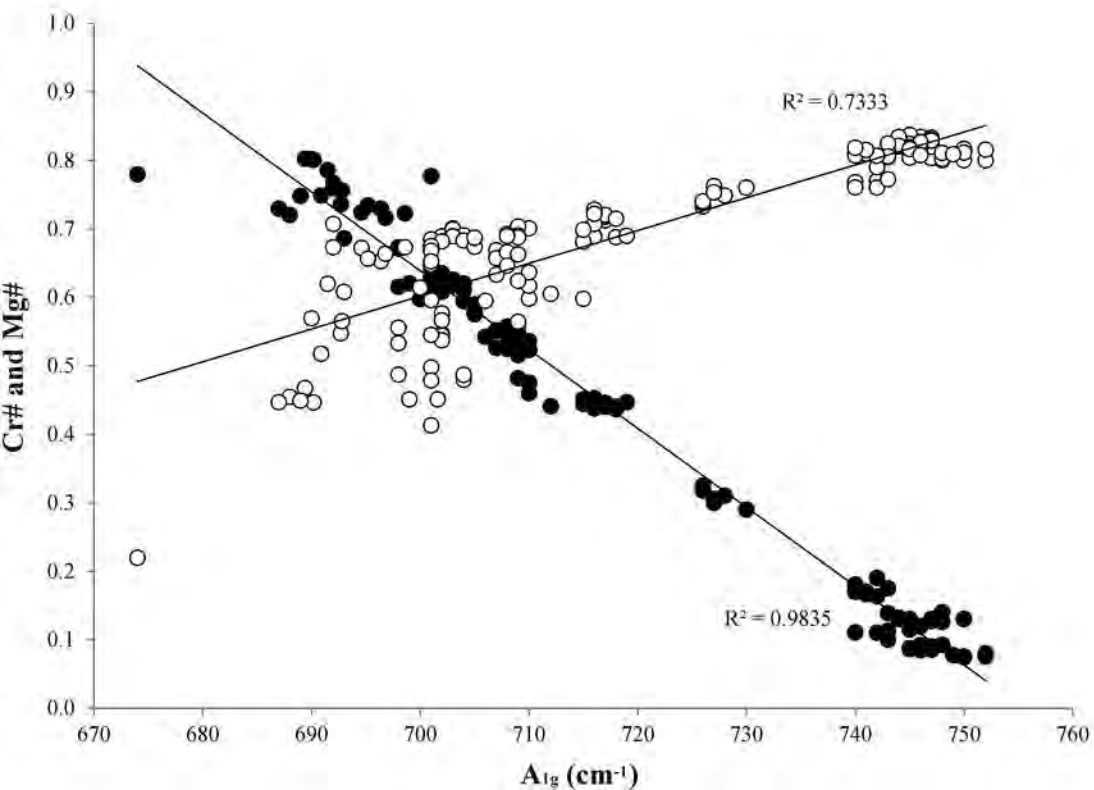


Table 1 Cell edge a_0 , oxygen positional parameter u , chemical analyses, cation distribution, Cr# (Cr/(Cr+Al) and Mg# (Mg/(Mg+Fe²⁺)), and inversion degree of the studied spinels. Complete structural and chemical parameters can be found in Lenaz et al. (2009a; 2010; 2012) and Derbyshire et al. (2013)

Sample	LB1A	BAR	LB10A	LB16A	LB3A	R2	R6
a_0	8.1219 (1)	8.1273 (1)	8.1307 (1)	8.1321 (2)	8.1542 (1)	8.1726 (2)	8.2359 (1)
u	0.26345 (5)	0.26251 (7)	0.26237 (7)	0.26338 (6)	0.26338 (8)	0.26351 (7)	0.26310 (5)
MgO	20.9 (1)	21.5 (1)	20.7 (1)	20.7 (2)	19.2 (2)	17.5 (1)	14.6 (3)
Al ₂ O ₃	60.1 (2)	56.7 (2)	57.1 (2)	56.3 (2)	50.2 (4)	44.7 (2)	33.9 (5)
Cr ₂ O ₃	7.51 (9)	8.6 (2)	11.2 (2)	12.4 (3)	17.4 (1)	24.5 (3)	32.5 (5)
FeO	9.2 (1)	8.1 (1)	8.9 (1)	9.1 (1)	10.4 (1)	12.2 (4)	15.3 (2)
Fe ₂ O ₃	1.7	2.7	1.8	1.7	3.0	0.53	2.81
T site							
Mg	0.698	0.668	0.613	0.717	0.734	0.654	0.586
Al	0.106	0.149	0.185	0.100	0.052	0.067	0.047
Fe ²⁺	0.161	0.127	0.172	0.156	0.148	0.266	0.351
Fe ³⁺	0.033	0.054	0.027	0.024	0.064	0.005	0.005
M site							
Mg	0.096	0.152	0.185	0.076	0.022	0.063	0.049
Al	1.706	1.619	1.551	1.613	1.521	1.380	1.114
Cr	0.152	0.172	0.228	0.252	0.364	0.532	0.752
Fe ²⁺	0.035	0.046	0.021	0.039	0.083	0.014	0.021
Fe ³⁺	0.000	0.000	0.007	0.010	0.000	0.005	0.050
Cr#	0.08	0.09	0.12	0.13	0.19	0.27	0.39
Mg#	0.80	0.83	0.81	0.80	0.77	0.72	0.63
i	0.139	0.203	0.212	0.124	0.116	0.072	0.052

Table 1

Sample	SWLB2	AV1	U392	C1	UDK5
a_0	8.2739 (2)	8.2691 (4)	8.3156 (2)	8.3134 (6)	8.3249 (2)
u	0.2630(2)	0.2629 (1)	0.26259 (7)	0.2623 (1)	0.26203 (8)
MgO	10.10(15)	11.0 (3)	9.0 (1)	11.1 (6)	12.3 (2)
Al_2O_3	20.55(20)	20.5 (4)	11.6 (2)	9.6 (1)	6.26 (9)
Cr_2O_3	44.54(49)	49.3 (7)	51.4 (4)	60.7 (6)	64.4 (4)
FeO	20.41(30)	18.7 (4)	19.8 (6)	16.8 (8)	13.6 (2)
Fe_2O_3	4.51	1.5	7.9	3.2	2.17 (9)
T site					
Mg	0.452	0.462	0.438	0.485	0.591
Al	0.015	0.045		0.017	0.016
Fe^{2+}	0.512	0.483	0.50	0.460	0.373
Fe^{3+}	0.009	0.002	0.046	0.030	0.012
M site					
Mg	0.020	0.042	0.005	0.045	0.018
Al	0.744	0.700	0.453	0.350	0.230
Cr	1.103	1.213	1.340	1.552	1.701
Fe^{2+}	0.020	0.004	0.040	0.000	0.005
Fe^{3+}	0.099	0.034	0.151	0.048	0.042
Cr#	0.59	0.62	0.75	0.81	0.87
Mg#	0.47	0.51	0.45	0.53	0.62
i	0.024	0.047	0.046	0.047	0.028